Journal of Catalysis **203,** 495–508 (2001)
doi:10.1006/jcat.2001.3344, available online at http://www.idealibrary.com on IDEAL®

High-Yield Butane to Maleic Anhydride Direct Oxidation on Vanadyl Pyrophosphate Supported on Heat-Conductive Materials: β-SiC, Si_3N_4, and BN

Marc J. Ledoux,*,[1] Claude Crouzet,* Cuong Pham-Huu,* Vincent Turines,* Kostantinos Kourtakis,† Patrick L. Mills,† and Jan J. Lerou‡

*Laboratoire des Matériaux, Surfaces et Procédés pour la Catalyse (LMSPC), UMR7515 du CNRS, ECPM, Université L. Pasteur, 25 Rue Becquerel, 67087 Strasbourg Cedex 2, France; †DuPont Company, Experimental Station, E304/A204, Wilmington, Delaware 19880-0262; and ‡Novodynamics, Inc., 123 North Ashley Street, Suite 210, Ann Arbor, Michigan 48104

Received April 23, 2001; revised July 9, 2001; accepted July 16, 2001

Both the preparation and the characterization of vanadyl pyrophosphate (VPO) supported on new heat-conductive ceramic supports (β-SiC, Si_3N_4, and BN) are described. These catalysts provide a very significant gain in maleic anhydride yield by reacting air and butane in a fixed-bed reactor, because of control of the catalyst surface temperature. The stable high maleic anhydride selectivity at high temperature, ensured by the presence of the support, allows the use of significantly high partial pressures of butane. In addition, the β-SiC support protects the catalyst against high-temperature accidental excursions.

Key Words: **heat-conductive catalyst support; vanadyl pyrophosphate (VPO); maleic anhydride; SiC; Si_3N_4; BN; oxidation; butane.**

1. INTRODUCTION

Much research effort has been devoted to the conversion of *n*-butane to maleic anhydride (MA) by one-step direct oxidation with air or oxygen. Most of this effort was dedicated to the characterization of the catalyst for this reaction, vanadyl pyrophosphate (VPO) (1–3), and to various process engineering aspects (4, 5). Vanadium, phosphorus, and oxygen can form a large number of distinct compounds that have been well characterized, e.g., α- and β-$VOPO_4$, γ-$VOPO_4$, $VOHPO_4$, $(VO)_2P_2O_7$, $VO(PO_3)_2$, and $VO(H_2PO_4)_2$. The most active catalytic phase is believed to be $(VO)_2P_2O_7$, which is also the predominant oxide phase in activated VPO catalysts. Nevertheless, VPO catalysts are usually referred to as "mixed oxides" in recognition of the probable presence of other oxide phases. VPO catalysts typically have V/P atomic ratios in the range 1 : 1 to 1 : 2 and have an average bulk vanadium oxidation state in the range 4.0–4.3.

[1] To whom all correspondence should be addressed. E-mail: ledoux@cournot.u-strasbg.fr.

The reaction mechanism was also investigated (6) and, if most of the authors agree on a Mars and Van Krevelen scheme (the labile oxygen from the solid being the oxidizing agent) (7), the step-by-step description and the nature of the intermediates are still not clear, and still in dispute. However, a better characterization of the catalyst or a better knowledge of the reaction mechanism will not resolve one of the main difficulties of this reaction which is its very high exothermicity, both for the production of the desired product, MA, and for its parallel parasitic full oxidation reaction (not to mention the reoxidation of the solid catalyst which is also exothermic):

$$C_4H_{10} + 7/2\,O_2 \rightarrow C_4H_2O_3 + 4H_2O, \qquad \Delta H = -276\ \text{kcal/mol},$$

$$C_4H_{10} + 13/2\,O_2 \rightarrow 4CO_2 + 5H_2O, \qquad \Delta H = -392\ \text{kcal/mol}.$$

This explains why recent developments in this important reaction were oriented mainly toward process studies dealing with the extraction of the heat generated from the reactor. The conventional process based on a fixed-bed system is limited by the diameter of the reactor and by the concentration of butane in the feed gas, which results in a low mass or volume yield. But because of the relative simplicity of the fixed-bed system, the large majority of MA is still produced through this operational system.

To overcome the restriction in yield, 15 years ago E. I. Dupont de Nemours developed a new process, similar to a cat-crack system and assuming the validity of the Mars and Van Krevelen mechanism, where the VPO catalyst and the gas feed brought into contact for a very short time in a riser tube, the solid catalyst then being separated from the other products, and reoxidized in a separate reactor before being reinjected into the flow. This process has several advantages over the conventional fixed-bed design:fast and easy extraction of heat by the flowing gas, high MA selectivity

0021-9517/01 $35.00

because of the absence of large concentrations of oxygen in direct contact with butane or MA, and a high concentration of butane (up to 40 vol% instead of 1–2 vol%) allowing a very high mass or volume yield. The two main drawbacks are (i) the need to reinforce the mechanical strength of the solid catalyst, made fragile by attrition due to the moving bed (this was solved by forming bulk vanadium phosphorus oxides in porous silica microspheres of a particular microstructure), and (ii) the complexity of the process control.

Both systems have in common the disadvantage of using bulk VPO catalyst, a costly material, relatively difficult to produce in a stable and active form. But the most inconvenient property of this material is its poor ability to conduct heat outside the reactor and to avoid hot spots on its surface because of its low thermal conductivity. Many attempts to economize the expensive VPO by dispersing it on different conventional supports (alumina, silica, TiO_2, etc.) have not been successful (8–10), mainly because of the strong interaction between the oxygen atoms of the support and the active phase, particularly during the activation step transforming the hemihydrate precursor into VPO. In addition, the thermal conductivity of these oxidic conventional supports is low (see Table 1) and large improvements in heat transfer are not expected during their use.

A few years ago large-specific-surface-area β-SiC (>20 m^2/g) was prepared via the "shape memory synthesis" (11, 12, 16). This material should be an excellent candidate to support VPO because of the absence of bulk oxygen in its structure, its ability to disperse different active phases demonstrated for other catalytic applications (13–15), and its high thermal conductivity, 146 to 270 W mol^{-1} K^{-1} (see Table 1), which should greatly contribute to the heat management of the reaction. The objective of this article is to show the successful application of this concept and its extension to other heat-conductive materials such as Si_3N_4 and BN.

TABLE 1

Thermal Conductivity of Some Catalyst Supports

Support	Thermal conductivity[a] (W m^{-1} K^{-1})
SiO_2 (silica)	0.015 to 1
Al_2O_3 (alumina)	1 to 8
SiC (silicon carbide)	146 to 270
Si_3N_4 (silicon nitride)	6
BN (boron nitride)	31

[a] Thermal conductivity is an anisotropic property in solid state, depending on the crystallographic direction of measurement and also on the allotropism of the solid. This explains the large range of values. This physical property is generally poorly documented in the literature. A very well documented article on the difficulty of measuring thermal conductivity in nonmetals had just been published by Srivastava (31).

2. EXPERIMENTAL

2.1. Catalyst Preparation

SiC was prepared in different shapes: fine powder (few micrometers), grains (0.5–1 mm), extrudates (1 cm long, 2–4 mm in diameter), or monoliths, according to the two methods already described and referred to by the generic term "shape memory synthesis." The first method (11, 12) is based on reaction of preformed activated charcoal with SiO vapor generated in a different chamber of the reactor; the second (16) is based on a mixture of carbon, oxygen-containing polymer, and Si fine powder, prehaped and heated under a neutral atmosphere. Because of the relatively low temperature of reaction, between 1200 and 1300°C, compared with the 1800°C necessary for the synthesis of conventional carborandum or α-SiC, the product obtained is maily β-SiC with a surface area varying between 20 and 120 m^2/g according to the reaction conditions. For the specific use of supporting VPO, the samples of β-SiC were selected in the range 25–35 m^2/g with a pore diameter distribution centered around 8–10 nm and no micropores (see later). For most of the tests reported here SiC was used in a grain form of 0.5–1 mm, which was the right dimension for the geometry of the catalytic reactor. Micronic powder and extrudates have been used on a larger scale in a riser or in a fixed-bed micropilot, respectively, but this is not reported here. The two variants of the β-SiC synthetic method were tested and similar results were obtained whatever the source. There is strong evidence that the surface of these SiCs displays a very peculiar composition: pure hydrophobic SiC outside the pores (low Miller index dense planes) and a thin layer ($\leq$2 nm) of a mixture of Si oxides and oxicarbides, hydrophilic, inside the pores, where the density of crystal defects is high (15, 17).

VPO was prepared according to the method published by Katsumoto and Marquis (18) where V_2O_5 was reduced to V_2O_4 by a mixture of benzyl alcohol and isobutanol, while the water formed by the reduction process was constantly extracted out of the solution via a conventional soxhlet device. Phosphoric acid was then added after the solution had been cooled down to room temperature and subsequently reheated to 120–130°C to form the so-called hemihydrate $(VO)HPO_4 \cdot 0.5H_2O$. This mixture was either treated to obtain a bulk VPO (tested against the best state-of-the-art industrial VPO) or modified by the addition of SiC powder, grains, or extrudates (19) with very critical control of the temperature. Then a drying procedure was conducted under partial vacuum until the mixture reached the consistency of a thick "mud." This "mud" was washed many times in hot water to extract the soluble unwanted $VO(H_2PO_4)_2$ phase. The remaining material was then dried at 200°C in air and crushed to recover the initial shape of the support, powder, grains, or extrudates. Different concentrations (5, 10, 27, and 60 wt% VPO) were prepared, and, after testing,

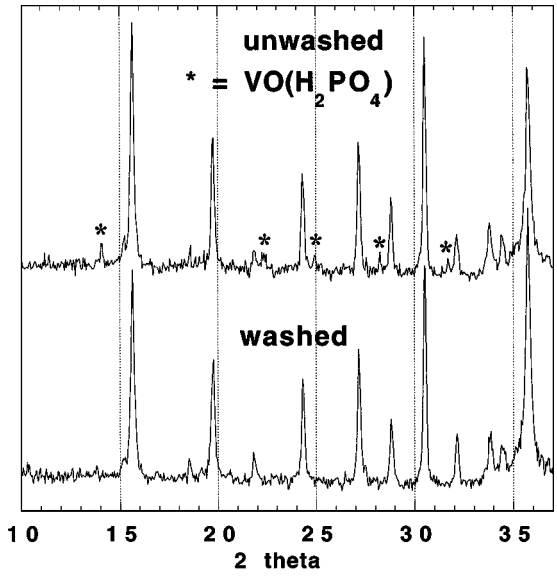

FIG. 1. Comparison of XRD patterns of washed and unwashed hemihydrate precursor.

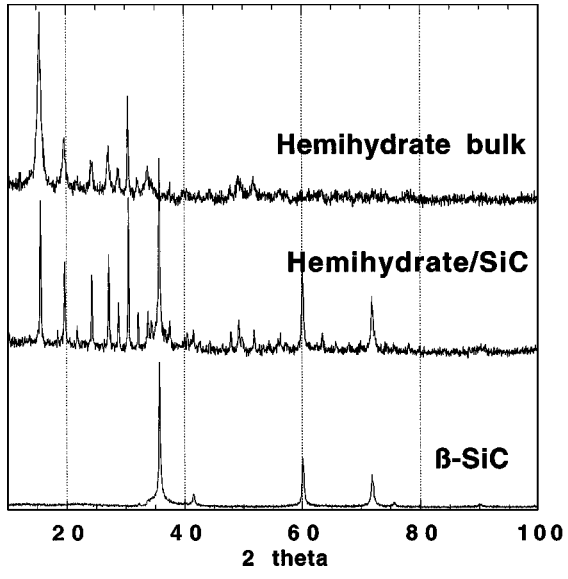

FIG. 2. Comparison of XRD patterns of bulk hemihydrate, β-SiC-supported hemihydrate, and pure β-SiC support.

27 wt% VPO was found to be the most active material, the 60 wt% VPO not being resistant to attrition and consequently not homogeneously set inside the reactor. Only the 27 wt% sample is considered in the following sections. The XRD diagrams of the unwashed and washed hemihydrate-supported precursor (Fig. 1) showed that the bands attributed to the unwanted phase, $VO(H_2PO_4)_2$, completely disappeared after washing. The XRD diagrams of the pure β-SiC support, of the bulk hemihydrate, and of the SiC-supported hemihydrate are shown for comparison in Fig. 2. XRD was performed with a Siemens D5000 diffractometer using Cu$K\alpha$ radiation over a large range of 2θ angles in a step-scan mode.

The washed supported hemihydrate was then subjected to activation to obtain the active VPO phase, according to the procedure already described by Katsumoto and Marquis (18). Many successive treatments in air or in mixtures of butane and air, at different temperatures, under different flow velocities, and at different durations were used (see Diagram 1). This entire procedure took about 100 h, and then the catalyst was run for about 500 h under reaction conditions (see later), and it was finally this material that was called stabilized VPO/SiC. This long process was adopted because it was thought to be the only way to obtain a stable catalyst in bulk form. It was found later that for the supported material it was not necessary to wait such a long time and that after the initial 100 h, the material had reached its highest activity and was stable. This was partly due to the fact that the supported material was activated at higher temperatures in the last phase, which probably accelerated the kinetics of the solid transformations. There were no detectable differences between the XRD diagrams of the activated and stabilized VPO/SiC reported in Fig. 3 as far as crystalline phases were concerned. However at low 2θ angles the background noise of the 500-h stabilized material was higher than that of the activated one (100 h) which was consistent with the existence of an amorphous phase possibly identified by HRTEM (see later). The BET surface of this stabilized material was 20 m^2/g instead of 17 m^2/g for the equivalent bulk VPO. The XRD diagrams of the activated

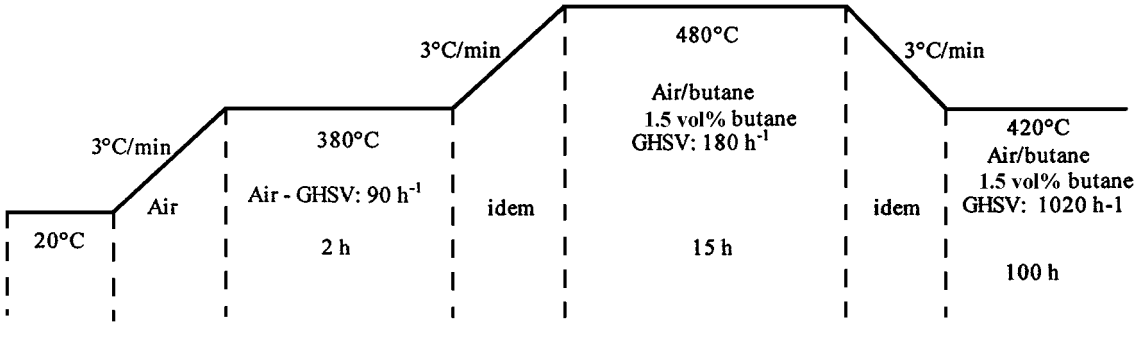

DIAGRAM 1. Sequences of hemihydrate activation used to obtain active VPO (last 100 h at 420°C for supported VPO and 380°C for bulk VPO).

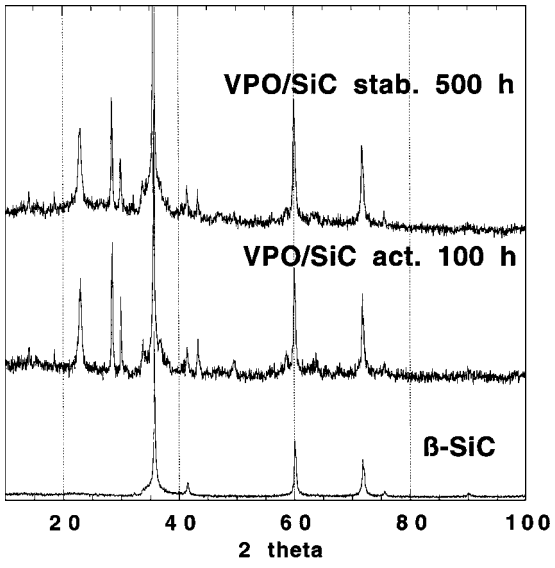

FIG. 3. Comparison of XRD patterns of activated (100 h) and stabilized (500 h) β-SiC-supported VPO.

catalysts (bulk and supported on SiC) are shown in Fig. 4. All the bands corresponding to VPO were clearly identified together with the bands of the SiC support in very good agreement with the literature (20, 21). No other unknown bands could be found. The elemental analysis of VPO-27 wt%/SiC gave a real concentration of 25.6 wt%, with an atomic P/V ratio equal to 1.06. The known anisotropic crystallinity of active VPO bulk (22) demonstrated by variations in the width of the peaks corresponding to different planes of diffraction was also observed on this supported catalyst (020 between 20 and 25° of 2Θ angles, larger than the other peaks). This confirmed that there were no negative interactions between the support and the VPO during the activation, as observed on oxidic supports, and that a "true" VPO was obtained. In addition this material was mechanically solid; no powder of unsupported VPO was ever found in the reactor after a long reaction time as was observed with supported material containing 60 wt% VPO. In the same way the use of carborundum or α-SiC as a support was not successful because even a small amount of VPO could not strongly stick to the support, the mechanical strength being very weak; just by shaking, solid VPO was quickly separated from α-SiC; this is in contradiction with the claims of Refs. (23–24). Conversely, even a long sonication could not extract VPO from β-SiC (30 wt% or below).

A similar process of impregnation and preparation was used to obtain 30 wt% VPO supported on silicon nitride, Si_3N_4, and boron nitride, BN (25). A fine powder of a commercial mixture of α- and β-Si_3N_4 (Goodfellow), with a BET surface area of 7 m^2/g, was impregnated in the same way as the β-SiC material. The complex XRD diagrams of the support, of the hemihydrate precursor, and of the final activated VPO are reported in Figs. 5 and 6. No obvious unknown bands could be detected on these diagrams; the supported hemihydrate on Si_3N_4 was less organized than the bulk form or than on the other supports. The mechanical stability of VPO/ Si_3N_4 (resistance to attrition during reaction or manipulation) was relatively good, but after a long reaction time some VPO powder was found in the reactor, meaning that the anchoring of VPO on the support was not as solid as for the β-SiC.

The use of BN as support revealed a much more complex system of interactions between the support and the active phase. BN (Alfa Johnson-Matthey), with a BET surface area of 8.4 m^2/g, was impregnated in the same way

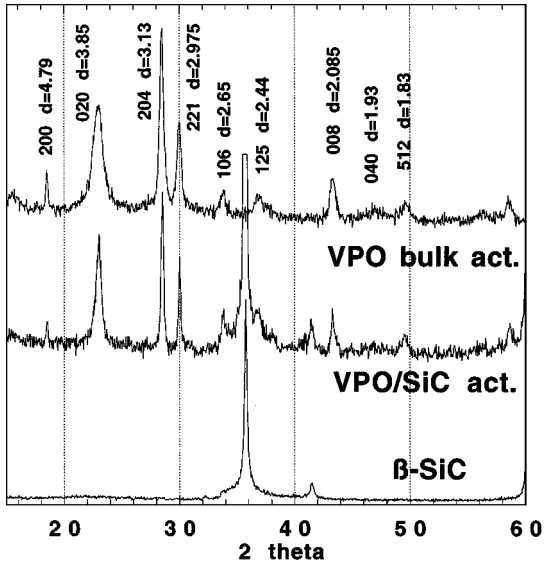

FIG. 4. Comparison of XRD patterns of bulk and β-SiC-supported activated VPO.

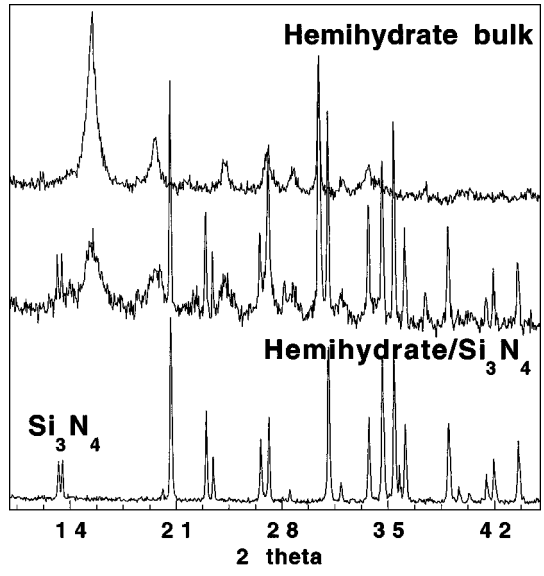

FIG. 5. Comparison of XRD patterns of bulk hemihydrate, Si_3N_4-supported hemihydrate, and pure Si_3N_4 support.

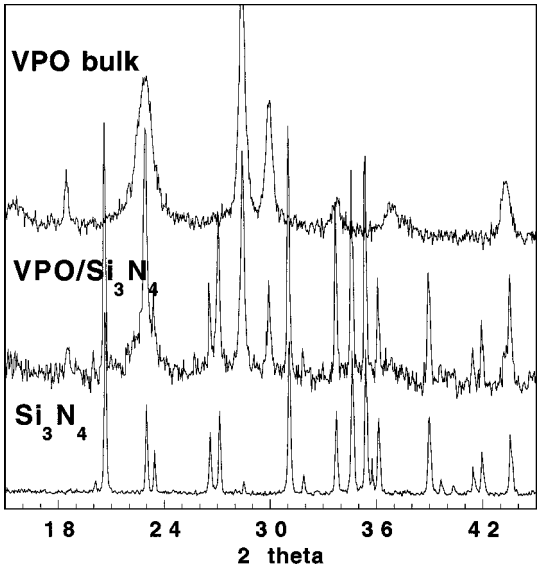

FIG. 6. Comparison of XRD patterns of bulk and Si_3N_4-supported activated VPO.

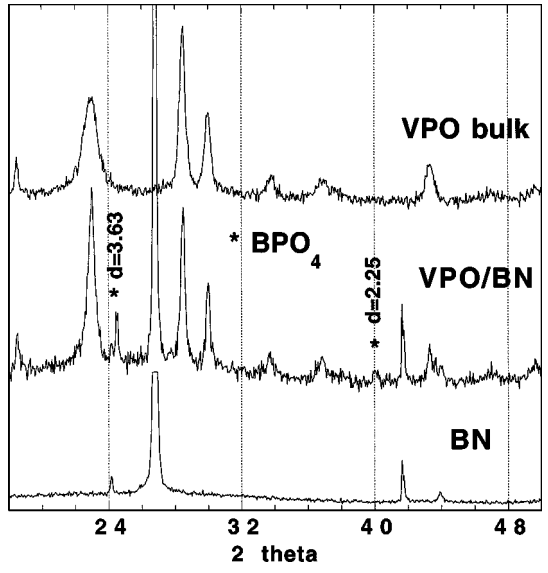

FIG. 8. Comparison of XRD patterns of bulk and BN-supported activated VPO.

as β-SiC or Si_3N_4. The XRD diagram between 18 and 34° of 2Θ angle of the supported precursor, 30 wt% hemihydrate (Fig. 7), revealed the presence of the expected bands corresponding to BN and to the hemihydrate, but four bands attributed to an unknown phase (corresponding to the following distances $d = 0.397$, 0.357, 0.316, and 0.282 nm) were also found. After checking in the literature and in the JCPDS database, it appeared that these peaks do not belong to any known phase. After activation the BN bands were still unchanged (Fig. 8), the VPO bands were also clearly observed, the three bands attributed to the unknown material had disappeared, and two bands of BPO_4 (tetragonal) were observed at $d = 0.363$ and 0.225 nm (26). The specific surface area of the stable catalyst was 12.6 m^2/g.

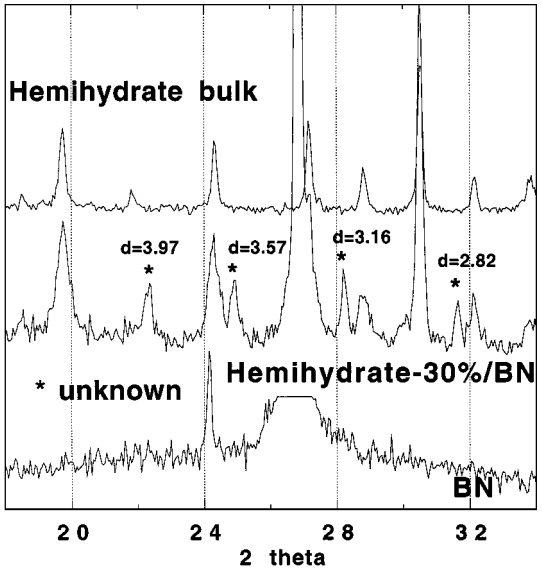

FIG. 7. Comparison of XRD patterns of bulk hemihydrate, BN-supported hemihydrate, and pure BN support.

2.2. *Catalytic Tests*

A detailed description of the micropilot used during this study has already been published (27). To summarize, the gas mixtures were prepared from six cylinders (Air Liquide, purity: N): pure butane, He/O_2 80/20 and 50/50, pure He, He/CH_4 60/40, and pure nitrogen. An all-metallic tube system, organized with 12 valves (two and three ways), plus four mass flow controllers, was connected to a fixed-bed reactor in silica–steel (steel tube with the internal wall coated with silica) which could contain up to 3 g of catalyst. The reactor was placed in an oven, with the temperature regulated at ±0.5°C from room temperature up to 750°C. The gas mixture flow could be varied from 1 to 100 ml/min in all requied butane/oxygen/helium ratios.

To get rid of the condensation of the maleic anhydride, all pipes and tubing after the reactor were enclosed in an oven heated above 210–220°C. The vent was bubbling in water to transform maleic anhydride into the corresponding acid and consequently avoid the formation of a solid block of anhydride at the outlet.

The on-line gas chromatograph was built around a Varian 3300 gas chromatograph (connected to a Compaq PC) equipped with two capillary columns heated from 50 to 110°C during the analyses. The first column, adapted to a TCD detector (He vector gas), Carboplot from Chrompack, was used for separation and analysis of the following products: He, O_2, CO, CH_4, and CO_2. The second column, adapted to a FID detector (H_2 vector gas), DB1 from JNW Scientific, was used for the separation and analysis of the following products: all hydrocarbons (CH_4,

butane, and butenes here) and oxygenated products (acetone, methacrolein, acrylic acid, crotonaldehyde, and maleic anhydride here). The injection of a known amount of CH_4 into the gas flow after the reactor allowed a very accurate carbon and oxygen mass balance to be reached ($100 \pm 1\%$) because this gas could be detected in both chromatograms and used as an internal standard; two independent loops were used to inject the products into the two columns. At each temperature the catalyst was stabilized over 3 h and then three measurements were performed in 2 h, the final value being the average of these three samplings. An experiment on the full temperature range necessitated a full week. At night the catalyst was left under the reacting flow at 380°C for bulk VPO and 420°C for supported VPOs, the initial temperatures of stabilization during 100 h (see Diagram 1).

2.3. Transmission Electron Microscopy

A Topcon EM002B UHR electron microscope operating at 200 keV for high-resolution transmission electron microscopy (HRTEM) was used. To prevent artifacts due to contamination, no solvents were ever added at any stage and samples were prepared by grinding the catalysts between glass plates and bringing the powder into contact with a holey carbon-coated copper grid. EDX microanalysis was used to provide the complementary data on elemental composition; the corresponding spectra are not reported. Great care was taken during the HRTEM experiments to avoid heating effects of the incident beam, VPO being extremely fragile and sensitive to the beam energy. In fact a blind procedure was adopted; i.e., about 30 photos were taken by switching the electron beam on and off for less than $\frac{1}{2}$ s and moving the focus distances step-by-step after each photo. The samples were stable enough to allow a magnification of 590,000 or more.

3. RESULTS AND DISCUSSION

3.1. Standard Bulk VPO

To obtain a fair comparison to study the effect of the support, two bulk VPOs, one laboratory-prepared according to the preparation procedure explained above and one industrial sample considered state of the art (Fig. 9) were tested. The state of the art sample was better crystallized as can be seen from the XRD data. They both gave similar activities and selectivities shown in Fig. 10, the state of the art sample being slightly better than the laboratory made sample (as usual !). Only the state of the art material will be used as a standard in the rest of this article, knowing, however, that all the supported catalysts were prepared like the lab-made bulk material. They were tested under the following conditions: catalyst mass $= 0.592 \pm 0.001$ g; catalyst volume $= 0.91 \pm 0.01$ cm^3; catalyst height $= 60 \pm 0.5$ mm; internal diameter $= 4.40$ mm ($\frac{1}{4}$ in.); total flow $= 36 \pm 0.5$ scm^3/min;

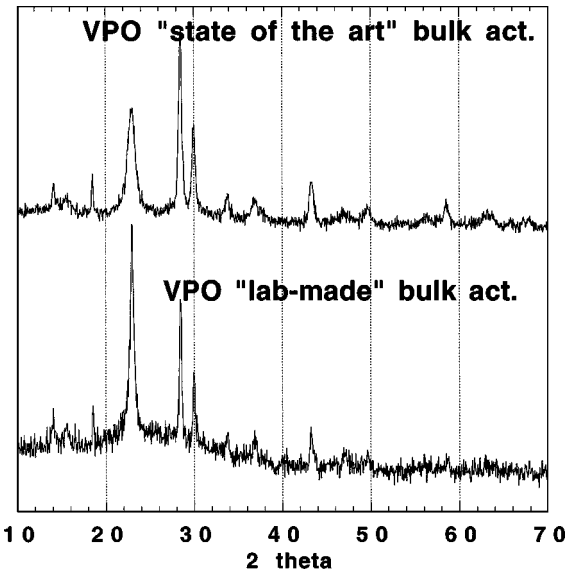

FIG. 9. Comparison of XRD patterns of "state of the art" and laboratory-made bulk activated VPO (100 h).

composition $= 11.0 \pm 0.05$ mol% butane, 16.5 ± 0.05 mol% oxygen, qsp. helium (calculated from gas chromatography); O_2/butane molar ratio $= 1.5$; contact time $= 1.52$ s. These were not the usual conditions for a fixed-bed system where, normally, the butane concentration should not exceed 2 mol%.

Up to 380°C, butane conversion regularly increased with temperature, accompanied by a relatively constant MA selectivity at around or above 80%. At 420°C butane conversion had leveled off and at the same time MA selectivity had sharply dropped, resulting in a severe decrease in MA yield. A more appropriate kinetic study would have probably shown that most of the by-products, CO and CO_2 and others, were produced by secondary reactions, i.e., the oxidation of MA formed in the first step (32). In Table 2 the distribution of these by-products obtained at 460°C is reported. Relatively large amounts of acetone, methacrolein, and acrylic acid were found. The optimum in terms of yield (24.4%) was observed at around 380°C; above this

TABLE 2

Selectivity of Oxygenated Molecules (Other Than Maleic Anhydride) Observed on Bulk VPO and VPO/β-SiC at 460°C

	Bulk VPO		VPO/SiC	
Product	Selectivity (%)	Yield (%)	Selectivity (%)	Yield (%)
Isobutane	0.00	0.00	0.07	0.03
(*trans* + *cis*)-2-Butene	0.16	0.05	0.08	0.04
Acetone	12.20	3.39	2.33	1.05
Methacrolein	1.14	0.37	2.32	1.04
Acrylic acid	9.19	3.01	4.74	2.13

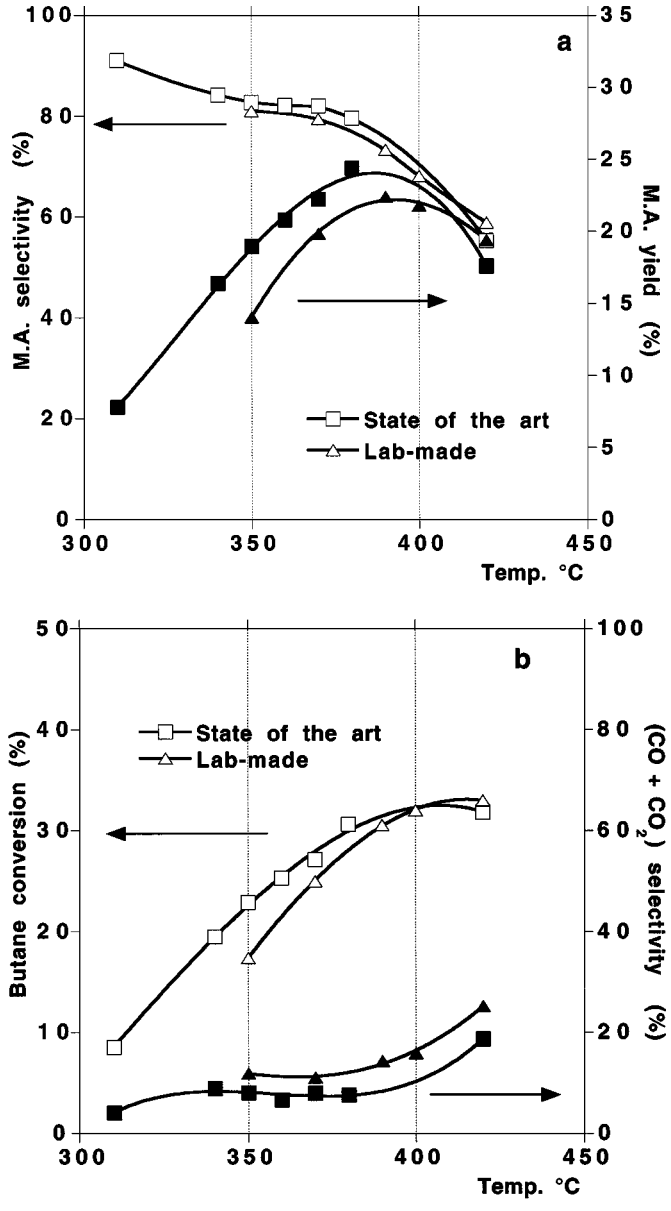

FIG. 10. Comparison of (a) MA selectivity and yield and (b) butane conversion and combustion selectivity, on "state of the art" and laboratory-made bulk VPO.

temperature the release of heat was too high to be evacuated from the catalyst surface, leading to combustion of MA.

3.2. VPO Supported on β-SiC

VPO-30 wt% supported on β-SiC (25.6 wt% after elemental analysis) was tested under the following conditions: catalyst mass = 0.400 ± 0.001 g; catalyst volume = 0.85 ± 0.01 cm^3; catalyst height = 40 ± 0.5 mm; internal diameter = 5.16 mm ($\frac{3}{8}$ in.); total flow = 35.0 ± 0.5 scm^3/min; composition = 12.9 ± 0.05 mol% butane, 18.6 ± 0.05 mol% oxygen, qsp. helium; O_2/butane molar ratio = 1.44; contact time = 1.04 s. These conditions were very close to those used for the bulk catalyst to make comparisons, with the exception of the contact time which was much shorter here (1.04 s instead of 1.52 s). It was always difficult to set conditions at exactly the same levels when the experiments were performed in a small reactor, with different solid materials (the densities being different), and with gas flows that could be accurately measured during the reaction only by gas chromatography. The shorter contact time in fact favored the performance of the supported catalyst.

The results (Fig. 11) were far from what was observed on bulk VPO. Instead of leveling off, butane conversion rose to 40% at 470°C, corresponding to a full conversion in oxygen (with a O_2/butane molar ratio of 1.44, the maximum theoretical conversion was 41%), without any strong negative effect on MA selectivity, which always remained above 70%. Consequently the MA yield increased to 27.4%, the total combustion into CO and CO_2 remaining relatively constant below 20% (not shown) and the other by-products at 470°C being mainly acetone, methacrolein, and acrylic acid (see Table 2). The fact that the β-SiC support showed no micropores below 5 nm in the pore size distribution centered around 12 nm (28) also favored MA selectivity. Too small pores could lead to an artificial increase in the contact time, particularly of the reaction products (i.e., MA), and thus to an increase in the unwanted total combustion selectivity.

Comparison of the apparent rate of butane conversion on the two catalysts (Fig. 12) showed that while on supported VPO this rate increased with temperature as expected for an activated catalytic reaction; on the bulk material above 380°C, this rate remained more or less constant. At low

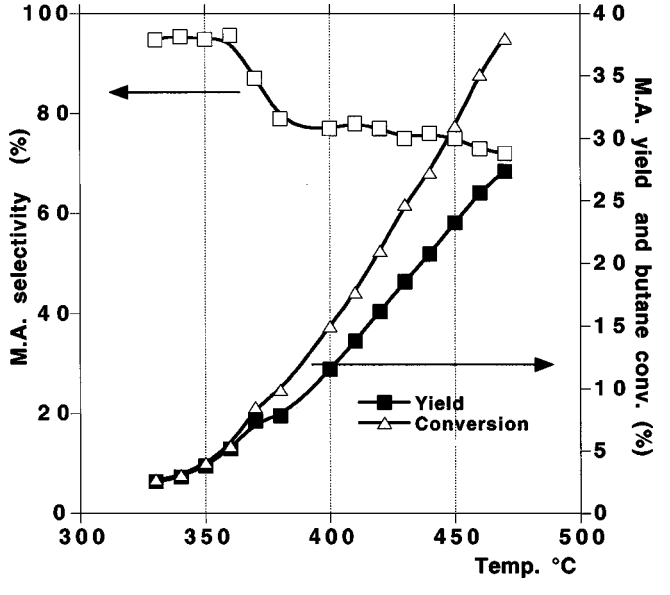

FIG. 11. MA selectivity and yield and butane conversion on β-SiC-supported VPO (30 wt%).

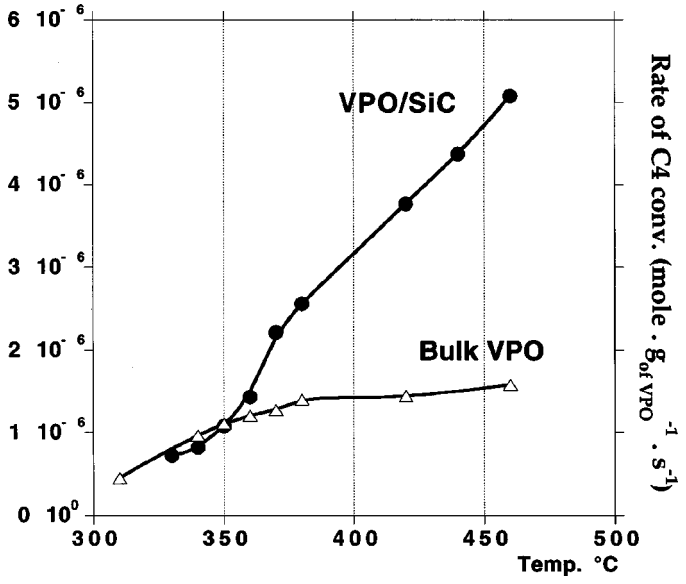

FIG. 12. Comparison of apparent rate of butane conversion on β-SiC-supported and bulk VPO, calculated per gram of VPO (full catalyst for bulk VPO and only active phase fraction for suported VPO).

temperatures (below 360°C) the rate evolved on an identical slope for the two catalyst, meaning that the same material was present on the active surface and that the heat generated by the reaction was properly extracted out of the reactor. The leveling off of the rate on bulk VPO at higher temperatures could be explained either because the surface of the catalyst (the active sites) was deactivated by a modification in the properties of the solid (phase transition, partial surface decomposition, etc.) or because this surface had reached too high a temperature, different from the macroscopic temperature of the reactor, by a local accumulation of heat (hot spots) and rendering negligible the small variation in macroscopic temperature. Both causes could also occur together. Sintering of the active phase could not be a cause of this phenomenon because it should not change the different selectivities as was observed. It was clear that on the β-SiC-supported catalyst the hypothesis that was set at the beginning seemed to be confirmed; i.e., the SiC support acted as a heat sink to avoid local surface hot spots and homogenize the temperature between the bulk and the surface.

To prove that it was not a simple effect of dilution and of a macroscopic heat transfer, the two catalysts, bulk VPO and VPO/β-SiC, were compared under the same experimental conditions with a mechanical mixture containing 30% bulk VPO and 70% pure β-SiC. The mechanical mixture behaved similarly to the bulk material (Fig. 13) in terms of MA selectivity (linear drop with temperature increase) and yield (a maximum slightly shifted toward higher temperature for the mixture, meaning a better macroscopic heat transfer). The effects observed on the supported material could not be reproduced by the mixture, emphasizing the role of the support and its interface with the active phase. If the heat conductivity of the suport was so important, the use of other heat conductive material should have the same effect on VPO activity.

3.3. *VPO Supported on Si_3N_4*

VPO-30 wt% supported on Si_3N_4 (150–250 μm) was tested under the folowing conditions: catalyst mass = 0.497 ± 0.001 g; catalyst volume = 0.71 ± 0.001 cm^3; catalyst height = 34 ± 0.5 mm; internal diameter = 5.16 mm ($\frac{3}{8}$ in.); total flow = 40.5 ± 0.5 scm^3/min; composition = 13.1 ± 0.05 mol% butane, 16.0 ± 0.05 mol% oxygen, qsp.

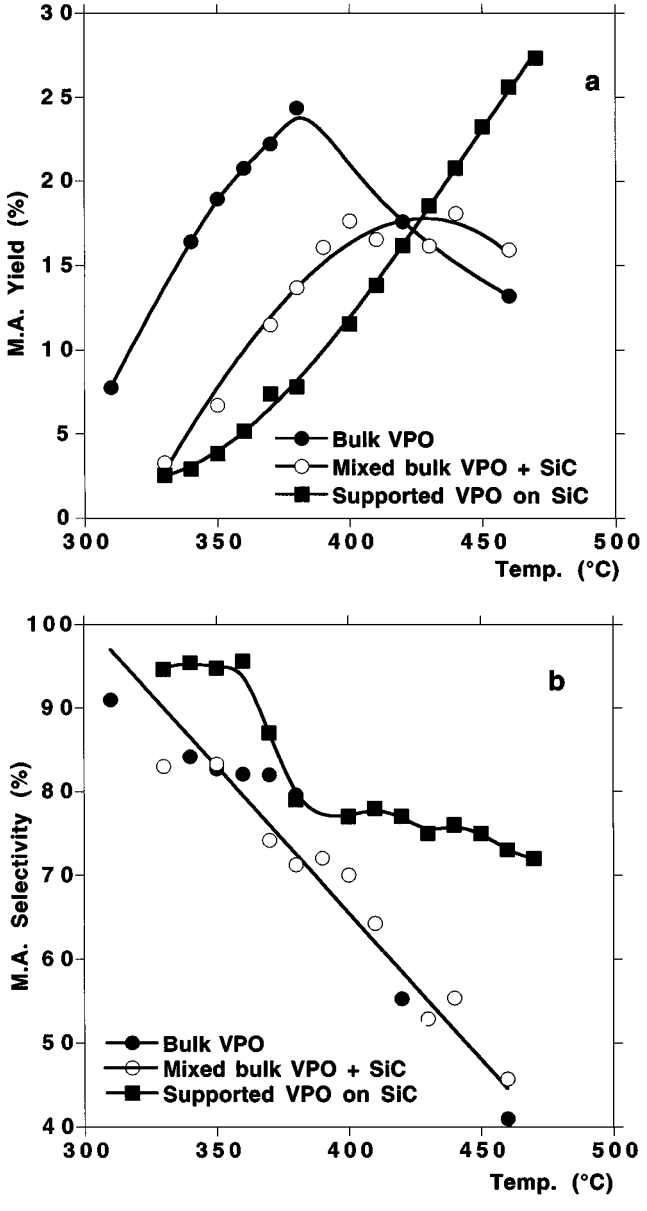

FIG. 13. Comparison of (a) MA yields and (b) MA selectivity, between β-SiC-supported VPO, mechanical mixture of β-SiC and VPO, and pure bulk VPO.

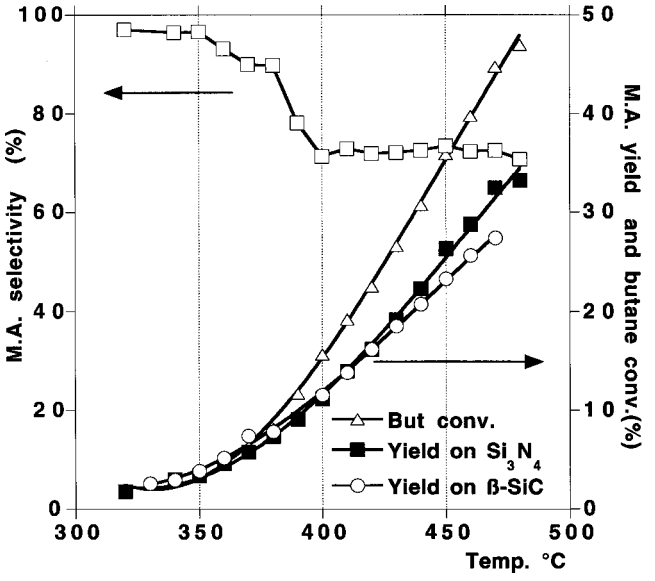

FIG. 14. MA selectivity and yield and butane conversion on Si_3N_4 supported VPO (30 wt%).

helium; O_2/butane molar ratio = 1.21; contact time = 1.04 s. These conditions were similar to the conditions used with the β-SiC support, particularly the contact time, which was the same.

The results (Fig. 14) were almost identical to what was found on VPO-30 wt% supported on β-SiC, meaning that the concept of heat conductive support was validated. There was, however, a difference: VPO was not as solidly fixed on the Si_3N_4 support as on β-SiC because after a long run (>500 h) some solid pure VPO was found in the reactor, mixed with the remaining catalyst. It was thus necessary to study the interface between the support and the active phase; BN support was for this purpose an easy case as shown below.

3.4. VPO Supported on BN

VPO-30 wt% supported on BN was tested under the following conditions: catalyst mass = 0.512 ± 0.001 g; catalyst volume = 0.93 ± 0.001 cm^3; catalyst height = 44.5 ± 0.5 mm; internal diameter = 5.16 mm ($\frac{3}{8}$ in.); total flow = 36.5 ± 0.5 scm^3/min; composition = 13.3 ± 0.05 mol% butane, 19.5 ± 0.05 mol% oxygen, qsp. helium; O_2/butane molar ratio = 1.47; contact time = 1.53 s.

As anticipated from the XRD study (Figs. 7 and 8) the catalyst supported on BN did not behave like the other VPO catalysts. The total oxidation ($CO + CO_2$) selectivity (Fig. 15b) remained relatively low at all temperatures, but the butane conversion and the MA selectivity were never as good as on β-SiC or Si_3N_4, providing one of the poorest MA yields (Fig. 15a). In fact, large amounts of by-products were formed at high temperatures when compared with the other catalysts, particularly acrylic acid (Fig. 16), resulting in a decrease in MA yield. A significant amount of phosphorus contained in the hemihydrate precursor and then in VPO had reacted with the support to form boron phosphate; consequently the activated VPO did not have the right P/V ratio necessary to obtain an active and selective phase for MA formation.

One could expect from pretreatment of the BN support with a water solution of phosphoric acid (P/B = 5 at%, 100°C to dryness) to saturate the surface of the support with phosphorus and to prevent further reactions with the supported active phase. The treated catalyst was tested under the same conditions as the untreated catalyst and provided the same results (Fig. 17) as already found on the β-SiC and Si_3N_4 supports, demonstrating again the role played by a heat conductive material.

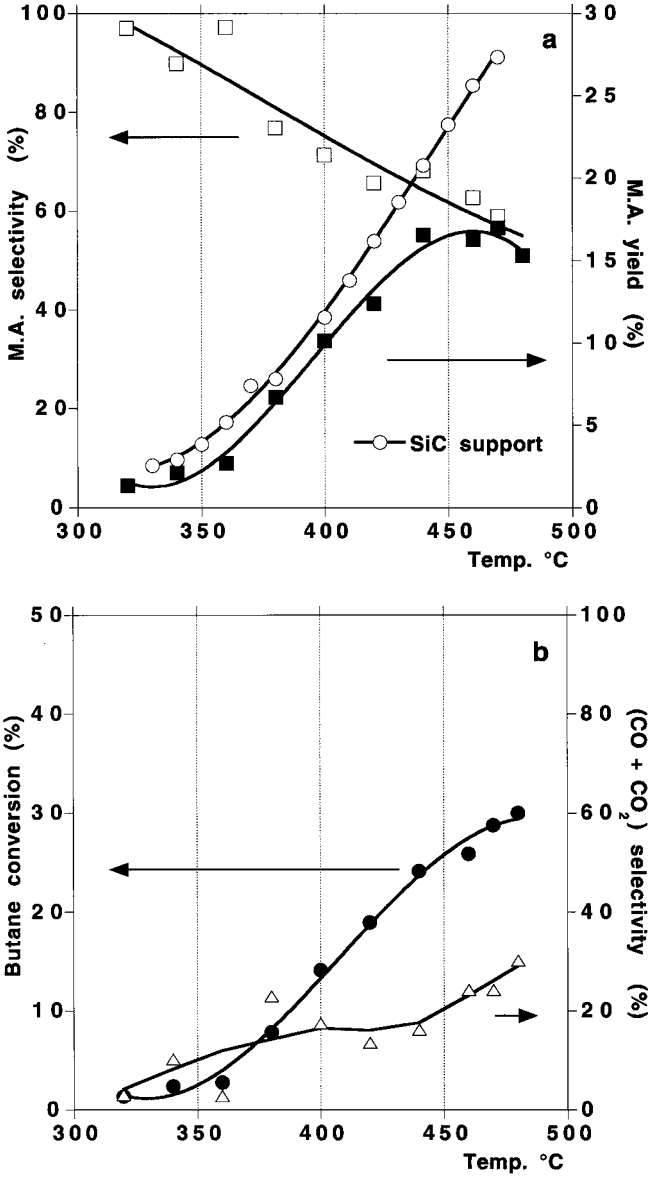

FIG. 15. Comparison of (a) MA selectivity and yield and (b) butane conversion and combustion selectivity on BN-supported VPO (30 wt%).

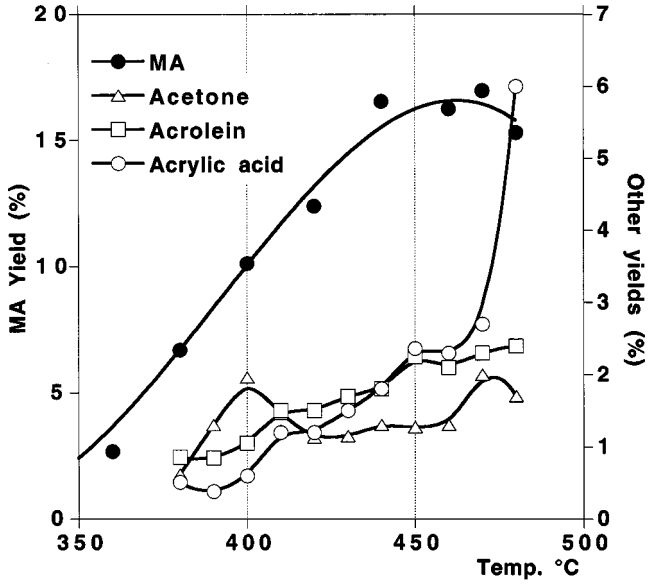

FIG. 16. Yields of by-products obtained on BN-supported VPO (30 wt%).

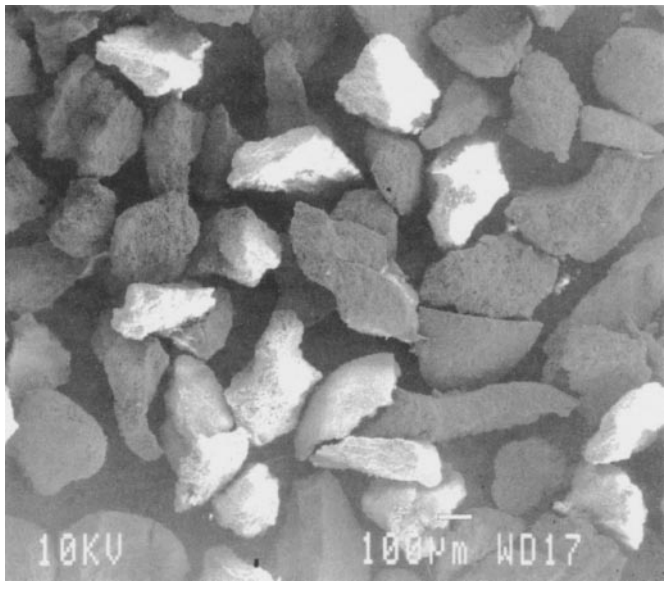

FIG. 18. Scanning electron micrograph of VPO/β-SiC.

3.5. SEM and TEM Analyses of the Interface

A scanning electron micrograph of VPO/β-SiC is reproduced in Fig. 18, showing that macroscopically VPO was well dispersed on the β-SiC grains without apparent heterogeneity in the material. Some grains were clearer than others because of charge effects. No crystalline structure other than VPO and β-SiC was observed by TEM. A well-crystallized VPO platelet supported on β-SiC is illustrated in Fig. 19a; the amorphous surface, particularly at the edge of the VPO slab, could be significant in understanding the real nature of the active site (30). These pictures were very difficult to obtain (see Experimental part) and when the electron beam was left irradiating the sample more than 20 to 30 s VPO started to become amorphous. Such a sample irradiated for 300 s is pictured in Fig. 19b; the lattice images of VPO had disappeared and only the lattice images of β-SiC (very stable under the beam) were clearly visible with amorphous VPO around (presence proved by EDX similar to Fig. 20b). Other EDX analyses performed on three different spots, on the support, on the interface between the active phase and the support, and on the active phase alone (Fig. 20a, 20b, and 20c), showed clearly that the interface between the active phase and the support contained a mixture of V, P, Si, and O (and probably C). This phase was probably acting as a glue, improving the resistance to phase separation and maintaining a high dispersion of the active VPO on the surface. A similar phenomenon was observed between VPO and BN.

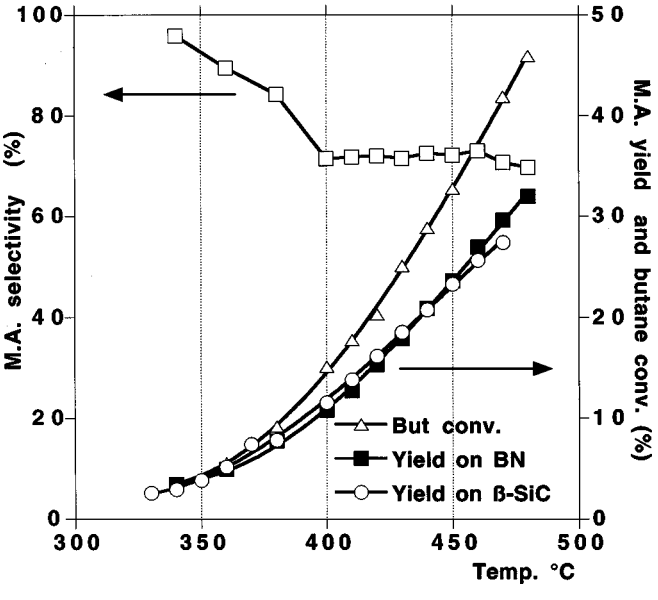

FIG. 17. MA selectivity and yield and butane conversion on VPO (30 wt%) supported on H_3PO_4-pretreated BN.

4. EXPECTED PROCESS IMPROVEMENTS DUE TO THE USE OF β-SIC SUPPORT

4.1. Increase in Volumic Yield

The catalytic activity of VPO/β-SiC reported in Section 3.2 (Fig. 11a) showed that complete exhaustion of oxygen was possible without loss in MA selectivity. But this total oxygen conversion limited the MA yield to a maximum of 27.4% at 470°C. The relative amount of oxygen should be largely increased to check if the volume yield (i.e., amount of MA produced by unit volume of catalyst) can reach values close to what can be obtained with a moving-bed system. If a conductive support, i.e., β-SiC, in a fixed-bed system could extract quickly enough the heat generated at the

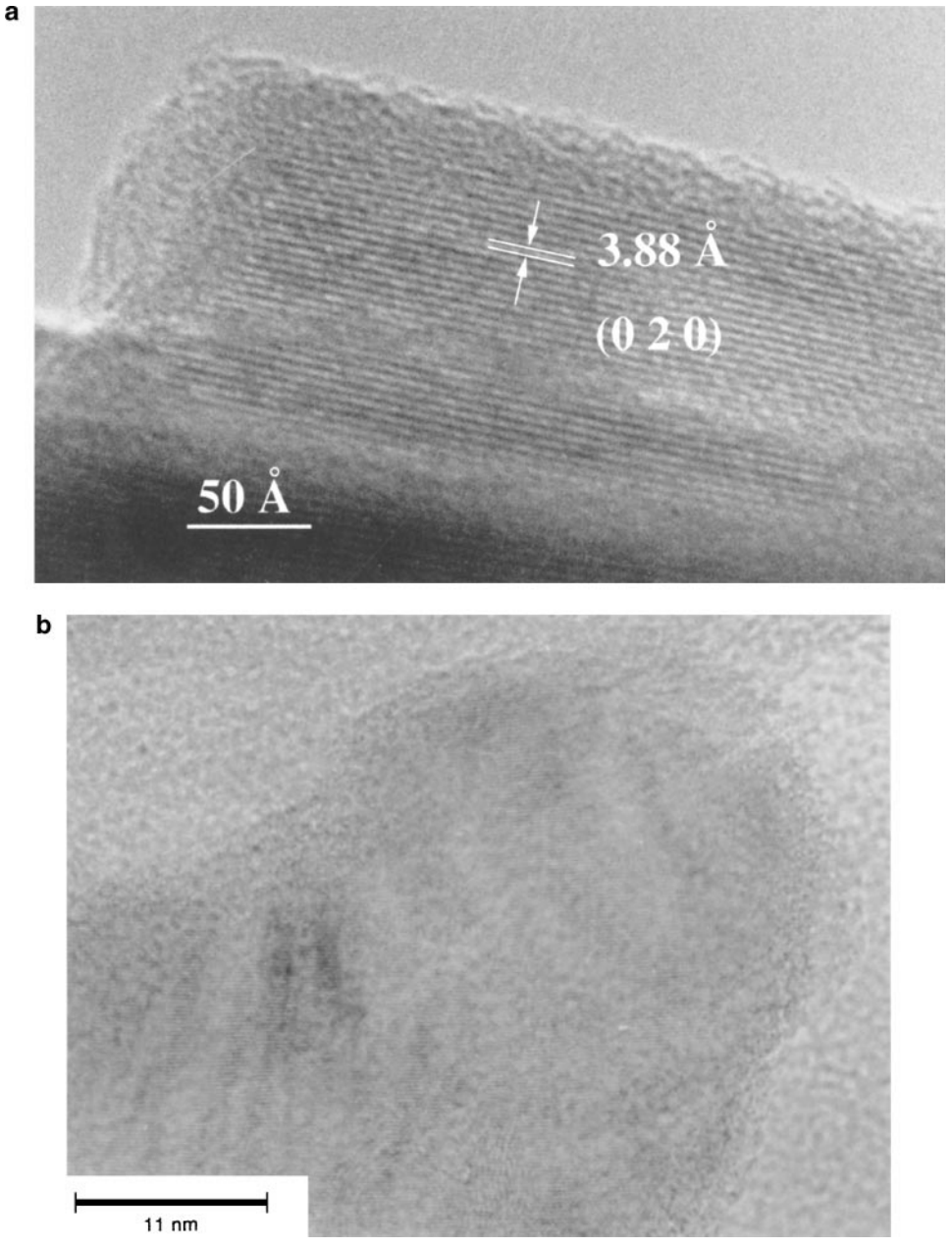

FIG. 19. High-resolution transmission electron micrographs of VPO/β-SiC. Electron beam irradiation: (a)<0.1 s, (b) >300 s.

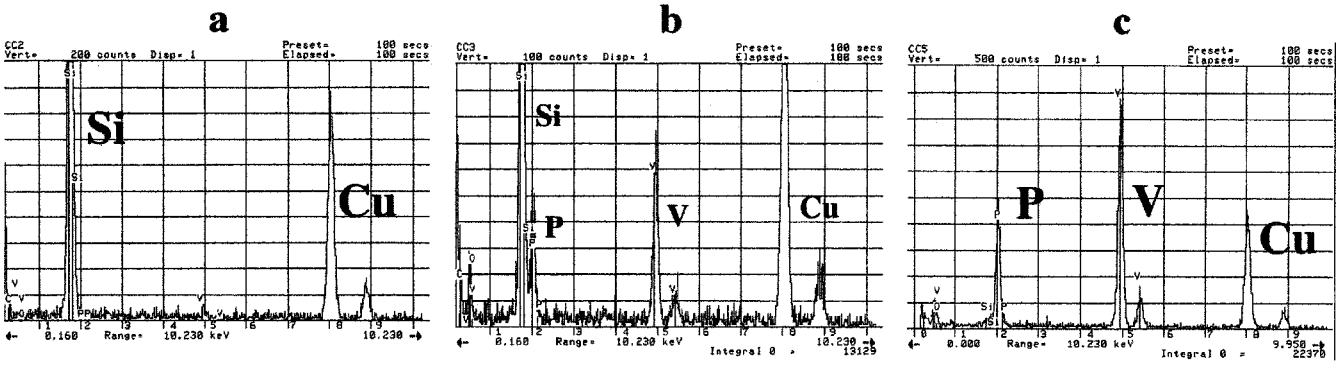

FIG. 20. EDAXS on (a) the β-SiC support, (b) the interphase, and (c) the VPO active phase.

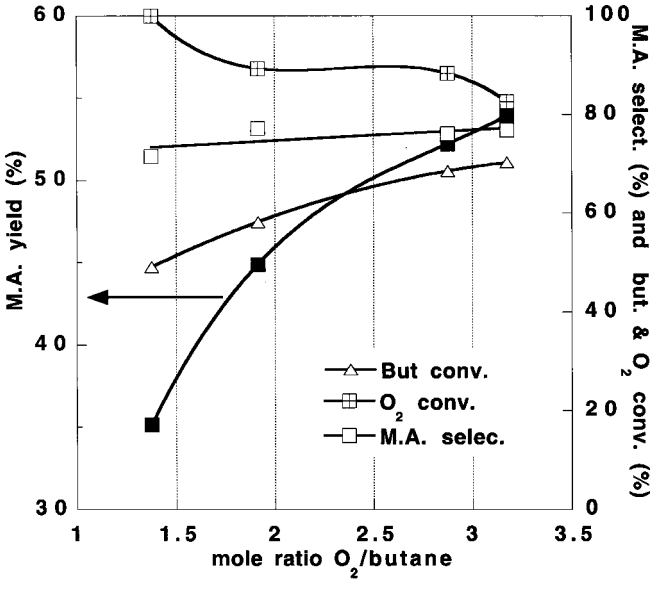

FIG. 21. Role of O_2/butane molar ratio in MA yield.

surface of the catalyst by the large amount of reacting butane, one should be able to obtain large volume yields much more easily than in a complex moving bed.

The initial conditions (Fig. 11a) were a O_2/butane molar ratio of 1.44 and a total flow of 35 cm^3/min. In the new test (Fig. 21), the catalyst temperature was set at $485 \pm 4°C$ and the butane flow at 2 cm^3/min for a constant volume of catalyst (0.602 g) (i.e., VHSV = 112.1 h^{-1}); only the O_2 flow was regularly increased. The O_2/butane molar ratio was increased from 1.38 to 3.17. The total flow was kept between 53 and 78 cm^3/min with a decreasing He (qsp) flow which, however, could not totally compensate the increase in O_2 flow. It was not possible to work at constant total flow as the O_2 and He flows were not completely independently controlled for safety reasons (no pure oxygen cylinders). This meant that the partial pressure of butane was slightly diminished at high O_2/butane ratio. It was important to keep the total flow in a relatively narrow range to maintain more or less constant heat transfer outside the reactor. As shown in Fig. 21, and as expected, butane conversion was no longer limited by the oxygen availability and increased from 50 to about 72%, this increase being kinetically handicapped by the decrease in butane partial pressure, if one assumes a positive order for the reaction. The MA selectivity remained high between 74 and 78% which as a consequence affected the MA yield which increased from 35 to 54%.

4.2. Improved Thermal Stability of the Catalyst

The thermal resistance of bulk VPO and β-SiC-supported VPO was tested according to the following procedure. After stabilization at 380°C for bulk VPO (500 h) and 480°C for supported VPO (100 h), the two catalysts were submitted to a series of temperature excursions, each of these excursions lasting 5 h, under the reactive flow. This high-temperature treatment was followed by a return to the reference temperature (380 and 480°C), the catalyst being left overnight (15 h) at this temperature to recover a stable regime; then, catalytic activity was remeasured under the usual conditions (see Section 3.1 for bulk and Section 4.1 for the supported material). The bulk VPO was treated at 430, 500, 550, 620, and 700°C, while the supported VPO was treated every 10°C from 480 to 560°C and then every 20°C up to 700°C. Such a treatment was designed to artificially reproduce an accidental heat excursion in an industrial system. According to this sequence it was also possible to precisely evaluate the upper limit of the heat stability of VPO under reactive flow.

The two catalysts remained stable even after treatment at 550°C (Fig. 22); for treatments above this temperature the bulk material could not be stabilized enough to measure any reproducible values of conversion or yield. The supported material was much more resistant and could withstand treatments up to 620°C with no problems; between 620 and 700°C it started to lose MA selectivity to the benefit of total combustion, meaning that above this temperature limit of 620°C the surface was irreversibly changing in nature to provide a new nonselective material, probably vanadyl phosphate (29), not able to return, after the 15 h of stabilization at 480°C, to the selective VPO phase. At a treatement temperature of 700°C both catalysts lost the total MA selectivity to give only full combustion. The possibility of recovering the initial MA selectivity from these dead materials was explored. The catalysts were submitted to the full process of the initial activation (see Diagram 1), but the bulk VPO was definitely unusable while the β-SiC-supported VPO was able to recover about a third (18%) of the initial MA yield (50%), another proof of its greater

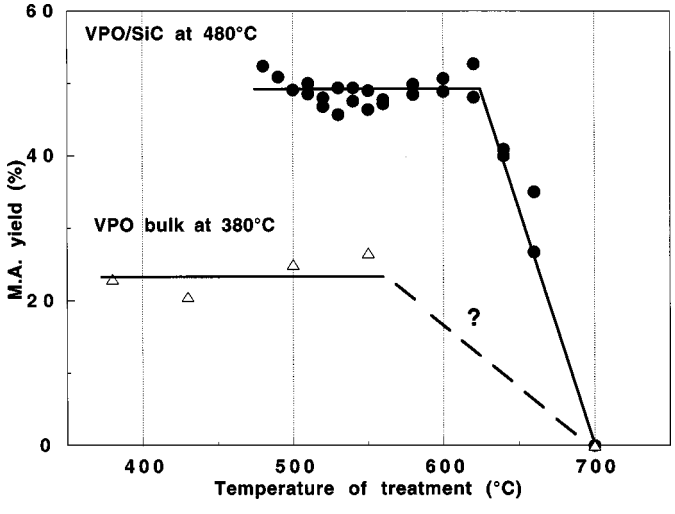

FIG. 22. Comparison of thermal stability between β-SiC-supported VPO and pure bulk VPO.

thermal stability due to the protective presence of the support.

5. CONCLUSION

A new generation of suports based on ceramics with high thermal conductivity and without oxygen atoms were prepared and tested to disperse the active $(VO)_2P_2O_7$ phase. The best example is a new relatively large specific surface area β-SiC (>20 m^2/g) prepared via the "shape memory synthesis." Conventional α-SiC (carborandum) of low specific surface area (<1 m^2/g), prepared via the Acheson process, was not able to disperse the active phase because of too little interaction between the two solids and particularly not able to avoid rapid separation of these two solids, α-SiC and VPO. The β-SiC-supported VPO proved to be a much better catalyst in terms of maleic anhydride selectivity and yield than its bulk equivalent, in a fixed-bed configuration of reactor. The ability of this ceramic to well disperse VPO was explained by the presence of an interphase (a glue) containing the V, P, Si, C, and O elements, which did not interfere with the formation of the active and selective VPO phase from the hemihydrate, $(VO)HPO_4 \cdot 0.5H_2O$. The real nature of this interphase still needs to be clarified. The high MA selectivity obtained on VPO/β-SiC was attributed to both the absence of microporosity on the support and, more importantly, to the heat sink role of this support avoiding the formation of hot spots on the catalytic sites and protecting the product, MA, from further oxidation into CO and CO_2.

The uses of other exotic heat conductive materials as support, such as Si_3N_4 and BN, proved the validity of the concept of heat transfer from the surface to the bulk of the catalyst, without taking into account the macroscopic transfer of heat outside the reactor, where conductive materials should also help, but was not proved in this study. The study performed on BN also showed the role of the interface acting as a glue, here probably BPO_4.

It was finally demonstrated, from an industrial point of view, that the presence of the β-SiC support could provide high volume yield of MA *per* volume of catalyst in a fixed-bed reactor because it was possible to work with relatively high concentrations of butane, contrary to what is normally possible with the conventional bulk catalyst. In addition, because of the good dispersion, a large fraction of the expensive unused internal part of the bulk active phase was replaced by cheap and light β-SiC support. The optimal amount of active phase was found at 30 wt% of the total composite. Finally, also demonstrated was the protective role of the support on the thermal stability of the reactive phase which was much more resistant to overheating accidents than the bulk material.

This new concept of heat control is currently being studied and used for other similar problems where nonoxidic conductive materials are potentially the answer to the difficulties that have been encountered in many applications.

ACKNOWLEDGMENTS

This work is the result of a long research collaboration between the LCMC and DuPont Experimental Station (U.S.) partially financed by DuPont Company. Heinz Hefter from DuPont Germany is thanked for this constant support. The Pechiney Company (France) is also thanked for its financial and scientific collaboration in the preparation of large amounts of β-SiC.

This article is dedicated to Claude Crouzet, one of the authors, who retired in July 2000 after having initiated and then developed the research on these new catalysts in the LCMC. All his former collaborators inside and outside the laboratory deeply acknowledge his remarkable achievements.

REFERENCES

1. Centi, G., *Catal. Today* **16**, 5 (1993).
2. Bordes, E., *Catal. Today* **16**, 27 (1993).
3. Sola, G. A., Pierini, B. T., and Petunchi, J. O., *Catal. Today* **15**, 537 (1992).
4. Wrobleski, J. W., Edwards, J. W., Graham, C. R., Keppel, R. A., and Raffelson, M. (Monsanto), U.S. Patent 4,562,68 (1985).
5. Contractor, R. M., Bergna, H. E., Horowitz, H. S., Blackstone, C. M., Malone, B., Torardi, C. C., Griffiths, B., Chowdhry, U., and Sleight, A. W., *Catal. Today* **1**, 49 (1987).
6. Centi, G., Trifiro, F., Ebner, J. R., and Franchetti, V., *Chem. Rev.* **88**, 55 (1988).
7. Mars, J., and van Krevelen, D. W., *Chem. Eng. Sci. Spec. Suppl.* **3**, 41 (1954).
8. Overbeek, R. A., Warringa, P. A., Crombag, M. J. D., Visser, L. M., van Dillen, A. J., and Geus, J. W., *Appl. Catal. A* **135**, 209 (1996), and references therein.
9. Overbeek, R. A., Pekelharing, A. R. C. J., van Dillen, A. J., and Geus, J. W., *Appl. Catal. A* **135**, 231 (1996).
10. Ruitenbeck, M., van Dillen, A. L., Koningberger, D. C., and Geus, J. W., *Stud. Surf. Sci. Catal.* **118**, 549 (1998), and references cited therein.
11. Ledoux, M. J., Hantzer, S., Pham-Huu, C., Guille, J., and Desanaux, M. P., *J. Catal.* **114**, 176 (1998).
12. Ledoux, M. J., Hantzer, S., Guille, J., and Dubots, D., U.S. Patent 4,914,070 (1990).
13. Pham-Huu, C., Marin, S., Ledoux, M. J., Weibel, M., Ehret, G., Benhaissa, M., Peschiera, E., and Guille, J., *Appl. Catal. B* **4**, 45 (1994).
14. Pham-Huu, C., Peschiera, E., Del Gallo, P., and Ledoux, M. J., *Appl. Catal. A* **132**, 77 (1995).
15. Keller, N., Pham-Huu, C., Crouzet, C., Ledoux, M. J., Savin-Poncet, S., Nougayrede, J. B., and Bousquet, J., *Catal. Today* **53**, 535 (1999).
16. Grindatto, B., and Prin, M. (Pechiney), European Patent 0,548,752 A (1992).
17. Keller, N., Thèse de Doctorat en Chimie, Univ. L. Pasteur, Strasbourg, 1999.
18. Katsumoto, K., and Marquis, D. M. (Chevron), U.S. Patent 4, 132, 670 (1979).
19. Ledoux, M. J., Crouzet, C., Bouchy, C., Kourtakis, K., Mills P. L., and Lerou, J. J. (Dupont), U.S. Patent Appl. & PCT CL-1097-P1 (1999).
20. Hodnett, B. K., *Catal. Rev. Sci. Eng.* **27**, 373 (1985).
21. Bordes, E., and Courtine, P., *J. Catal.* **57**, 236 (1979).
22. Sananes, M. T., Tuel, A., Hutchings, G. J., and Volta, J. C., *J. Catal.* **148**, 395 (1994).

23. Kerr, R. O. (Petro Pex Chem. Corp.), U.S. Patent 3,156,705 (1964).
24. Schneider, R. A. (Chevron), U.S. Patent 3,864,280 (1975).
25. Crouzet, C., Bouchy, C., Kourtakis, K., Ledoux, M. J., and Lerou, J. J. (Dupont), U.S. Patent Appl. & PCT CL-1299 (1999).
26. JCPDS—International Centre for Diffraction Data, No. 34-0132 (1997).
27. Meunier, F., Delporte, P., Heinrich, B., Bouchy, C., Crouzet, C., Pham-Huu, C., Panissod, P., Lerou, J. J., Mills, P. L., and Ledoux, M. J., *J. Catal.* **169**, 33 (1997).
28. Keller, N., Pham-Huu, C., Roy, S., Ledoux, M. J., Estournes, C., and Guille, J., *J. Mater. Sci.* **3**, 3189 (1999).
29. Bordes, E., *Catal. Today* **3**, 163 (1988).
30. Hutchings, G. J., Bartley, J. K., Webster, J. M., Lopez-Sanchez, J. A., Gilbert, D. J., Kiely, C. J., Carley, A. F., Howdle, S. M., Sajip, S., Caldarelli, S., Rhodes, C., Volta, J. C., and Poliakoff, M., *J. Catal.* **197**, 232 (2001).
31. Srivastava, G. P., *MRS Bull.* **26**, 445 (2001).
32. Roy, S., Dudukovic, M. P., and Mills, P. L., *Catal. Today* **61**, 73 (2000), and references cited therein.